Interaction-controlled Brownian motion in a tilted periodic potential

Mykhaylo Evstigneev,* Sebastian von Gehlen, and Peter Reimann
Fakultät für Physik, Universität Bielefeld, 33615 Bielefeld, Germany
(Received 17 September 2008; published 14 January 2009)

The drift and diffusion of a few interacting, overdamped Brownian particles in a tilted periodic potential are studied analytically and numerically. Both quantities exhibit a complex multipeaked structure as a function of the equilibrium interparticle separation. Upon variation of the interaction strength, both drift and diffusion may exhibit a nonmonotonic, resonancelike behavior.

DOI: 10.1103/PhysRevE.79.011116 PACS number(s): 05.40.−a, 05.60.−k, 02.50.Ey

I. INTRODUCTION

The drift and diffusion of a single Brownian particle in a tilted washboard potential represent a long-studied problem in nonequilibrium statistical physics. It is of relevance in a number of diverse research areas and belongs to the rare problems which can be solved analytically. The expression for the velocity in the overdamped limit was obtained by Stratonovich some 50 years ago [1], while an analytic result for the diffusion coefficient was derived relatively recently [2].

In many physical situations one deals not with single Brownian particles, but with arrays of a finite number of interacting particles finding themselves in a periodic potential and acted upon by some external force. The problem of coupled Brownian particles in a periodic structure is important in a large number of fields. Examples include molecular motors [3–14], friction [15–21], diffusion of dimers on surfaces [22–29], diffusion of colloidal particles [30–32], DNA translocation through a nanopore [33], charge density waves [34,35], and arrays of Josephson junctions [36,37], to name but a few. Many-particle systems may exhibit some features not found in the single-particle counterparts, such as phase transitions, spontaneous ratchet effects, and negative mobility [38].

In the present work, we study the behavior of a one-dimensional array of a finite, typically small, number of overdamped Brownian particles in a tilted periodic potential. Our system is closely related to the one investigated in Ref. [29]. The difference of our model from the one considered in that work is that, on the one hand, we restrict ourselves to the case of the overdamped dynamics, while the authors of [29] consider a more general case of arbitrary damping; on the other hand, in Ref. [29], the motion of a pair of interacting particles is studied, whereas we do not impose any restriction on the number of particles in the array. By numerically solving the underlying equations of motion, as well as by using asymptotic analytic results for the velocity and diffusion coefficient at low and high coupling strength, we report and qualitatively explain additional features of the system's dynamics. Namely, we show that both velocity and diffusion coefficient can be maximized with respect to the coupling strength. Furthermore, we find that these characteristics exhibit an interesting multipeaked dependence on the equilibrium interparticle separation.

II. MODEL

We consider an array of N interacting overdamped Brownian particles in a one-dimensional, periodic potential,

$$U(x) = U(x+L), \tag{1}$$

tilted by a homogeneous, static force F. The equation of motion for the coordinate x_i of the ith particle is

$$\eta\dot{x}_i(t) = -U'(x_i(t)) + F - \frac{\partial W(x_1(t), \ldots, x_N(t))}{\partial x_i} + \sqrt{2\eta T}\xi_i(t). \tag{2}$$

Here, η is the friction coefficient and thermal fluctuations of energy T are modeled as usual by Gaussian noises $\xi_i(t)$ with

$$\langle \xi_i(t) \rangle = 0, \quad \langle \xi_i(t)\xi_j(s) \rangle = \delta_{ij}\delta(t-s). \tag{3}$$

The meaning of the coordinates x_i depends on the concrete problem at hand. For instance, in the studies [3–33] of molecular motors, sliding friction, diffusion of dimers and colloids, and DNA translocation, they represent the physical coordinates of the respective components, such as heads of the molecular motors, surface atoms, colloidal particles, DNA segments, etc. In the models of pinned charge density waves [34,35], they represent the local phases thereof. Finally, in the arrays of Josephson junctions [36,37], they stand for the phase differences of the superconducting order parameter between both sides of the barrier.

The interaction potential $W(x_1, \ldots, x_N)$ in (2) is assumed to be confining and translation invariant,

$$W(x_1 + b, \ldots, x_N + b) = W(x_1, \ldots, x_N), \tag{4}$$

$$W(x_1, \ldots, x_N) \to \infty \quad \text{if } |x_i - x_j| \to \infty \tag{5}$$

for all real b and all indices $i \neq j$. We furthermore assume that W has a single minimum, such that in the absence of all other forces, the particles are regularly spaced with period a at the positions

$$x_i^{\min} = ia + x - (N+1)a/2, \tag{6}$$

relative to their common center of mass

*mykhaylo@physik.uni-bielefeld.de

$$x := \frac{1}{N}\sum_{i=1}^{N} x_i. \tag{7}$$

An example is provided by the all-to-all harmonic coupling

$$W(\{x_i\}) = \frac{\kappa}{2}\sum_{i=1}^{N} (x_i - x_i^{\min})^2, \tag{8}$$

where $x_i^{\min}$ is related to the center of mass via Eq. (6). Physically, this interaction may thus be viewed, e.g., as emerging due to a rigid (but massless) "backbone," to which the "particles" x_i are attached via springs at regular distances a. Such systems quite naturally arise, e.g., in the context of molecular motors [3,4,6,13] and atomic friction [15,16,18–21].

Our goal is to find the average velocity and diffusion coefficient of the center of mass (7) of the N-particle system (2),

$$v := \lim_{t\to\infty} \frac{\langle x(t)\rangle}{t}, \quad D := \lim_{t\to\infty} \frac{\langle x^2(t)\rangle - \langle x(t)\rangle^2}{2t}, \tag{9}$$

and, in particular, their dependence upon the most important system parameters. Unlike the majority of previous related works, we assume free rather than periodic boundary conditions and, most importantly, our main focus will not be on the large-N limit but rather on quite small particle numbers.

Due to the internal degrees of freedom of the many-particle system (2), this problem is considerably more complex than the single-particle counterpart. Therefore, an analytical treatment will be possible only in the situations when the many-particle problem can be approximately reduced to a single-particle one, namely, for asymptotically weak and strong coupling. These analytical results will be derived in the next section. In Sec. IV, we will present the results of our numerical simulations of Eq. (2), as well as of the analytic approximations, to demonstrate and discuss some interesting peculiarities of the diffusion of the many-particle system.

III. ANALYTICAL RESULTS

For a single, overdamped Brownian particle in a tilted periodic potential [$N=1$ in Eqs. (2)–(7)] the mean velocity from (9) is given by the exact analytical formula [1,2]

$$v_1(\{u_n\},T) = \frac{1 - e^{-FL/T}}{\displaystyle\int_{x_0}^{x_0+L} \frac{dx}{L} I_{\pm}(x)}, \tag{10}$$

for any choice of the reference point x_0 and of the indices $\pm$ in

$$I_{\pm}(x) := \frac{T}{\eta}\int_0^L dz \exp\left(\pm\frac{U(x) - U(x\mp z) - F(x-z)}{T}\right). \tag{11}$$

The subscript 1 in Eq. (10) indicates that the result applies to a single particle and, for later convenience, we have explicitly indicated its dependence on temperature T and the Fourier components u_n of the periodic potential:

$$U(x) = \sum_{n=-\infty}^{\infty} u_n e^{inqx}, \quad u_{-n} = u_n^*, \quad q := \frac{2\pi}{L}. \tag{12}$$

Likewise, the single-particle diffusion coefficient from Eq. (9) is given by the exact analytical formula [2]

$$D_1(\{u_n\},T) = \frac{T}{\eta}\frac{\displaystyle\int_{x_0}^{x_0+L} \frac{dx}{L} I_{\pm}(x) I_{+}(x) I_{-}(x)}{\left(\displaystyle\int_{x_0}^{x_0+L} \frac{dx}{L} I_{\pm}(x)\right)^3}. \tag{13}$$

A. Weak-coupling limit

In the absence of the interaction potential W in (2), the N individual particles are statistically independent of each other and thus $\langle x_i(t)x_j(t)\rangle = \langle x_i(t)\rangle\langle x_j(t)\rangle$ for all $i \neq j$ and all times t. Exploiting this fact after introducing Eq. (7) into (9) readily yields the following result for the velocity and diffusion coefficient of the center of mass:

$$v = v_1(\{u_n\},T), \quad D = \frac{D_1(\{u_n\},T)}{N}. \tag{14}$$

Turning to asymptotically weak but finite interactions, it is intuitively quite plausible that the concomitant modifications of velocity and diffusion of the center of mass will also be asymptotically small. Formally, this means that the limits of vanishing interaction in (2) and of large times in (9) commute. In other words, we expect the results (14) to remain approximately valid for sufficiently weak interaction potentials W. While we have no rigorous proof of this conjecture, it is in full agreement with our extensive numerical explorations.

B. Strong-coupling limit

For asymptotically strong coupling, the individual particles maintain fixed positions with respects to their common center of mass, namely, $x_i^{\min}$ from Eq. (6). Hence we expect that the center of mass behaves like one single, "big" Brownian particle with some appropriately renormalized potential and thermal noise.

To work out this program, it is convenient to change to the shifted particle coordinates

$$\tilde{x}_i := x_i - ia \tag{15}$$

and their corresponding center of mass

$$\tilde{x} := \frac{1}{N}\sum_{i=1}^{N} \tilde{x}_i = x - (N+1)a/2, \tag{16}$$

where the last equality follows from (7) and (15). In the new coordinates, the equations of motion (2) assume the form

$$\eta\dot{\tilde{x}}_i(t) = -U'(\tilde{x}_i(t) + ia) + F - \frac{\partial W(\{\tilde{x}_j(t) + ja\})}{\partial \tilde{x}_i} + \sqrt{2\eta T}\xi_i(t). \tag{17}$$

Next, we sum over all i and divide by N, yielding $\eta\dot{\tilde{x}}$ on the left-hand side. On the right-hand side, the sum over the in-

teraction terms vanishes, as follows by differentiating (4) with respect to b. The last arithmetic average of the N independent, δ-correlated Gaussian noises $\xi_i(t)$ results in $N^{-1/2}$ times a single, δ-correlated Gaussian noise $\xi(t)$. Specifically, for asymptotically strong coupling it follows from $x_i=x_i^{\min}$ (see above) together with (6), (15), and (16) that $\tilde{x}_i=\tilde{x}$. All in all, we thus find in the strong-coupling limit that

$$\eta\dot{\tilde{x}}(t) = -\tilde{U}(\tilde{x}(t)) + F + \sqrt{2\eta T/N}\xi(t), \tag{18}$$

with an effective potential

$$\tilde{U}(x) := \frac{1}{N}\sum_{i=1}^{N} U(x+ia) \tag{19}$$

whose Fourier components are related to those of the bare potential in (12) via

$$\tilde{U}(x) = \sum_{n=-\infty}^{\infty} \tilde{u}_n e^{inqx}, \tag{20}$$

$$\tilde{u}_n = u_n \frac{e^{inqa}}{N}\frac{1-e^{iqnNa}}{1-e^{inqa}}. \tag{21}$$

In view of (16) one readily sees that the resulting drift and diffusion for $\tilde{x}$ will be the same as those for x from (9). Since (18) represents an effective single-particle dynamics for $\tilde{x}$, we can employ (10) and (13) to infer for the velocity and the diffusion coefficient in the strong-coupling limit:

$$v = v_1\left(\{\tilde{u}_n\}, \frac{T}{N}\right), \quad D = D_1\left(\{\tilde{u}_n\}, \frac{T}{N}\right). \tag{22}$$

These expressions become exact for rigidly coupled particles. For large but finite coupling strengths, one can approximately account for the resulting small but fast fluctuations of the individual particle positions around their accompanying "strong-coupling equilibria" by integrating over those fluctuations [23]. We do not present the corresponding formulas, as we have found that all interesting effects are already captured by our leading-order expressions (22).

C. Symmetries

Focusing on the specific interaction potential from (8), the equations of motion (17) for the shifted particle coordinates (15) can be rewritten (for arbitrary κ) in the form

$$\eta\dot{\tilde{x}}_i = -U'(\tilde{x}_i + ia) + F - \kappa(\tilde{x}_i - \tilde{x}) + \sqrt{2\eta T}\xi_i(t). \tag{23}$$

It follows that the velocity and diffusion coefficient remain unchanged if the equilibrium interparticle distance a is increased by an integer multiple of the lattice constant L of the potential: $v(a+kL)=v(a)$, $D(a+kL)=D(a)$. Furthermore, changing a to $-a$ is equivalent to renumbering the particles in the reverse order, again leaving the physical properties, such as v and D, unchanged. This implies the following symmetry property of the quantities of interest:

$$v(kL \pm a) = v(a), \quad D(kL \pm a) = D(a) \tag{24}$$

for any integer k.

We remark that the symmetry property (24) is valid for interactions (23) of arbitrary strength κ. Moreover, the periodic potential $U(x)$ may be arbitrary, and, in particular, does not need to be spatially symmetric.

IV. NUMERICAL RESULTS

To evaluate the velocity and diffusion coefficient from numerical simulation of Eq. (2), direct application of the definition (9) is somewhat inconvenient. This is so because, in general, the numerical effort to reach good convergence is quite high and, in particular, the time necessary for convergence of the quantities $\langle x(t)\rangle/t$ and $\langle[x(t)-\langle x(t)\rangle]^2\rangle/2t$ is different for differently chosen parameter values. Therefore, we have employed an alternative numerical procedure based on the relations from [2] between v and D and the first two moments of the time necessary for the center of mass to cover the distance kL, where k is an integer:

$$v = \frac{kL}{\langle t(x_0 \to x_0 + kL)\rangle},$$

$$D = \frac{(kL)^2}{2}\frac{\langle t^2(x_0 \to x_0 + kL)\rangle - \langle t(x_0 \to x_0 + kL)\rangle^2}{\langle t(x_0 \to x_0 + kL)\rangle^3}. \tag{25}$$

These relations are strictly valid if the transitions by the distance kL are statistically independent events [2]; in other words, information about the state of the system before the transition is lost after the transition. This is the case for one-particle systems for any value of k; hence, for a single particle, one can take its smallest value, $k=1$. For a system consisting of several Brownian particles, this is not the case, because the system has "memory" in the form of the internal degrees of freedom, making the consecutive transitions not statistically independent. Therefore, additional care should be taken to make sure that this is a negligible effect. Numerical application of the formula above yielded identical (within statistical error) results for v and D for $k=1$ and 2 for all parameter values tested. This means that such memory effects are indeed negligible, and one can apply the relation above, taking $k=1$. For each data point, the results were based on at least 1000 transitions by L.

For simplicity, we focus on the specific potential

$$U(x) = \frac{\Delta U}{2}\cos\frac{2\pi x}{L} \tag{26}$$

with fixed corrugation depth $\Delta U=10T$ and unit periodicity, $L=1$. In terms of the Fourier expansion from (12), the only nonzero Fourier components are thus $u_1=u_{-1}=\Delta U/4$. Both the thermal energy T and the friction coefficient η are also set to unity. Furthermore, we use the all-to-all harmonic coupling from (23).

A. Dependence on the tilt

Figure 1 shows the dependence of velocity and diffusion coefficient on the bias for the asymptotic cases considered in Sec. III [see Eqs. (14) and (22)], and for the intermediate cases $\kappa=100$ and 200. Depicted are results for the dimer

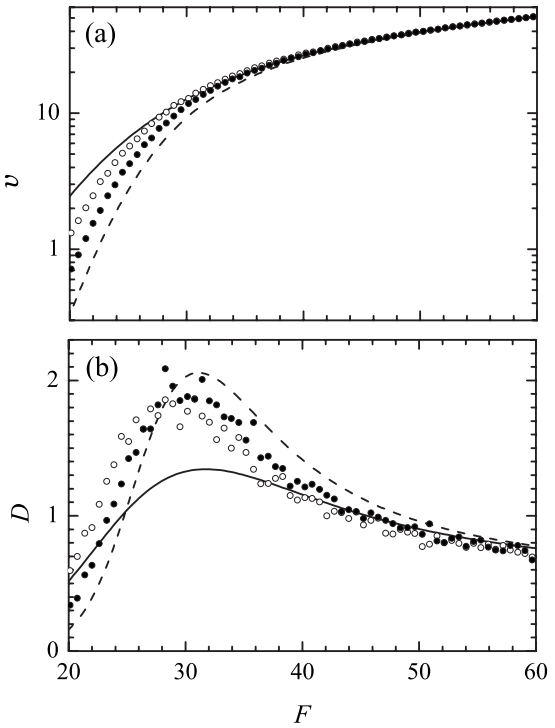

FIG. 1. Velocity and diffusion coefficient (9) vs tilt F for a dimer ($N=2$), satisfying (2) with (8) and (26), $\eta=T=L=1$, $\Delta U=10$, vanishing equilibrium interparticle separation ($a=0$), and different values of the coupling constant κ. According to (27), the critical tilt is $F_c=31.4\ldots$. Dashed lines: Analytical results (14) for asymptotically small κ. Solid lines: Analytical results (22) for asymptotically large κ. Filled and empty circles: Numerical results for $\kappa=100$ and 200, respectively. The numerical uncertainty is quantified by the small erratic deviations from a smooth behavior. For still smaller and larger κ values (not shown), the numerically obtained results approach the corresponding analytical asymptotics.

($N=2$), while other values of N (not shown) produced similar curves.

For all values of the coupling constant, two regimes can be distinguished. At high value of the bias F, the spatial modulation of the potential is negligible. In this regime, the velocity asymptotically approaches F/η and the diffusion coefficient converges toward $T/(\eta N)$. In the opposite regime of small bias F, the dynamics is governed by thermally activated transitions between local potential wells, leading for both the velocity and the diffusion to very small values with an approximately Arrhenius-type, exponential increase with F. These two regimes are separated by the critical bias

$$F_c = \pi \Delta U/L, \tag{27}$$

at which the barriers of the tilted periodic potential just disappear, degenerating into flat regions.

At $F \approx F_c$, the diffusion coefficient exhibits a maximum. This maximum can be understood as follows. Instead of a single system, let us consider an ensemble of many noninteracting replicas of the system. If the tilt exceeds the value F_c, all members of the ensemble are sliding down with approximately the same velocity around F/η. On the other hand, for F values much smaller than F_c, most of the members are trapped in the potential minima, with only a small fraction performing a thermally activated interwell jump at each moment of time. But in the critically tilted case, a notable part of the replicas will remain in the flat regions of the potential and have zero velocity (up to small thermal fluctuations) while the others will perform a downhill motion with a large velocity. This means that the spreading of the ensemble will proceed faster than in the overcritically tilted regime, when all the replicas are in the running state, and also faster than in the subcritical case, when the interwell transitions are rare events.

Conversely, if one considers velocity and diffusion coefficient as functions of the barrier height ΔU (or, equivalently, the value of F_c) at a fixed nonzero F value, then the former will be a decreasing function of the potential amplitude with a maximum $v_{\max}=F/\eta$ at $\Delta U=0$, and the latter will exhibit a nonmonotonic behavior. Namely, the diffusion coefficient will grow with ΔU until the corresponding critical force F_c from Eq. (27) will reach the value of the tilt F, and then start to decrease upon further increase of the potential amplitude in the regime of subcritical tilt.

B. Dependence on the coupling strength

So far our discussion has been mainly focused on the situation when the many-particle array could be described as an effective one-particle system with properly renormalized potential and temperature. Yet, finite coupling strengths are expected to lead to additional interesting effects which are captured neither by the weak-coupling (14) nor strong-coupling (22) asymptotics.

To study these effects, we now turn to the dependence of the velocity and diffusion coefficient on the coupling strength. Figure 2 illustrates the results of numerical simulation of Eq. (2). As before, we focus on the case of a dimer, $N=2$, since the results for larger particle numbers were qualitatively the same.

Figure 2 shows the velocity and diffusion coefficient for a dimer in the potential with the same parameters as before, tilted with the force $F=22\approx 0.7F_c$. The two sets of curves correspond to the dimer rest length $a=0$ (filled circles) and $L/2$ (open circles).

For small coupling constant κ, the diffusion properties of the dimer practically do not depend on the rest length and are given by Eq. (14). At large κ, on the other hand, the system behaves as a single Brownian particle in the effective potential (19), whose modulation depth equals 0 for $a=L/2$. Therefore, the velocity of the dimer with the rest length $a=L/2$ increases monotonically from the single-particle value given by Eq. (14) to the value F/η. On the other hand, for $a=0$, the amplitude of the effective potential is the same as in the noninteracting case, i.e., ΔU, but the effective temperature in (18) is twice as small. Therefore, the probability of the interwell transitions become exponentially suppressed due to the Arrhenius factor, and the velocity drops from the same initial value to a smaller value.

Interestingly, in between the two extremes, the velocity of the dimer of zero rest length as a function of the coupling strength develops a maximum at some intermediate κ value

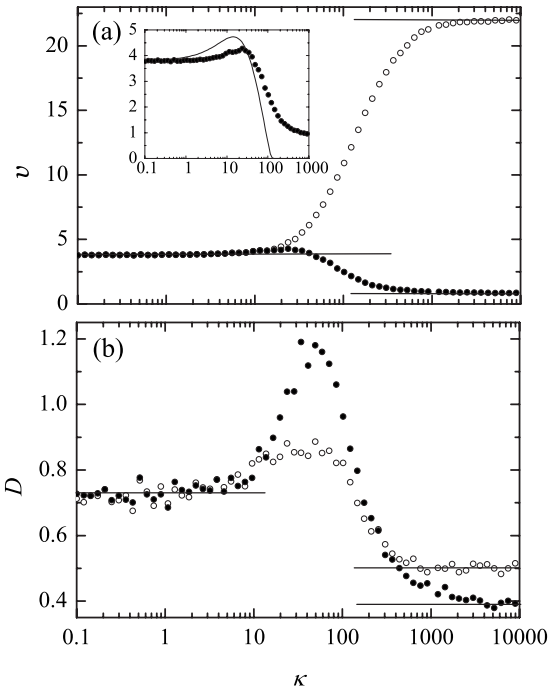

FIG. 2. Velocity and diffusion coefficient vs coupling constant κ for the same system as in Fig. 1 with a fixed tilt $F=22$ and a dimer rest length of $a=0$ (filled circles) and $L/2$ (empty circles). Horizontal lines correspond to the analytical results for asymptotically small and large κ from (14) and (22), respectively. The inset in (a) shows the velocity for $a=0$ together with the results of the analytic approximation (29).

comparable to the second derivative of the host potential at a minimum [see the inset in Fig. 2(a)]. This behavior is reminiscent of the results reported in Ref. [7], although the underlying physical mechanism is quite different. The nature of this nonmonotonicity is the correlated character of the jumps of the two dimer components between the minima of the tilted periodic potential. We propose that the following simplified picture captures the main qualitative features of the effect.

The motion essentially proceeds in steps as shown in Fig. 3. For a small but finite κ, the "downhill" transition of the dimer consists of two stages. In the first stage, the system

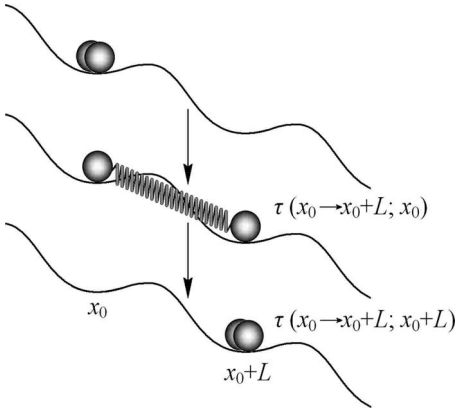

FIG. 3. Model of dimer motion in a tilted periodic potential.

finds itself in the "ground state," where both components are found within one of the minima, x_0, of the tilted periodic potential $U(x)-Fx$. At some point, one of the particles, the "leader," performs a thermally activated transition into the next minimum, while the second particle, the "follower," remains in the previous potential well. The characteristic time for this process can be estimated as the mean first passage time $\tau(x_i \to x_f; z)$ for one particle to go from the initial position x_i to the final position $x_f > x_i$, provided that the other particle is at a fixed position z:

$$\tau(x_i \to x_f; z) = \frac{\eta}{T} \int_{x_i}^{x_f} dx\, e^{[U(x)-Fx+(\kappa/2)(x-z)^2]/T} \times \int_{-\infty}^{x} dy\, e^{-[U(y)-Fy+(\kappa/2)(y-z)^2]/T}. \quad (28)$$

The average time of entrance from the "ground state" to the "first excited state" in Fig. 3 is approximately $\tau(x_0 \to x_0 + L; x_0)$. Similarly, the transition of the "follower" into the next potential well takes approximately $\tau(x_0 \to x_0+L; x_0+L)$. The resulting velocity is inversely proportional to the average time to cover one spatial period L:

$$v = \frac{2L}{\tau(x_0 \to x_0 + L; x_0) + \tau(x_0 \to x_0 + L; x_0 + L)}, \quad (29)$$

where the factor 2 in the numerator accounts for the fact that any of the two particles can assume the role of the leader.

The formula (29) is rather crude, as it does not capture many important features. In particular, it assumes that one of the particles remains stationary during the second particle's transition into the next minimum. Furthermore, it approximates the true positions of the particles in different potential wells with the respective minima of the tilted periodic potential. Finally, this approach neglects the possibility of multiple transitions performed by either particle.

Despite all these approximations, Eq. (29) still reproduces qualitatively correctly the behavior of velocity with the coupling constant, in particular, the fact that v is maximized at some κ value (see Fig. 2). Accordingly, we can understand this maximum as resulting from the competition between two effects: on the one hand, the presence of the follower hinders the transition of the leader into the next potential well, increasing $\tau(x_0 \to x_0+L; x_0)$; on the other hand, once the leader makes such a transition into the next well, it is easier for the follower to get there, thus reducing the second contribution to the total time, $\tau(x_0 \to x_0+L; x_0+L)$.

It is interesting to observe that the diffusion coefficient is also maximized at the coupling strength of the order of the second derivative of the tilted periodic potential at a minimum. Similar to the diffusion enhancement with respect to the tilt (see Sec. IV A), the diffusion maximum marks the boundary between the two modes of the dimer motion characterized by substantially different velocities—the uncorrelated jumps realized at weak coupling and completely correlated motion at large κ. At the intermediate coupling constants, both modes can be realized, meaning that in a

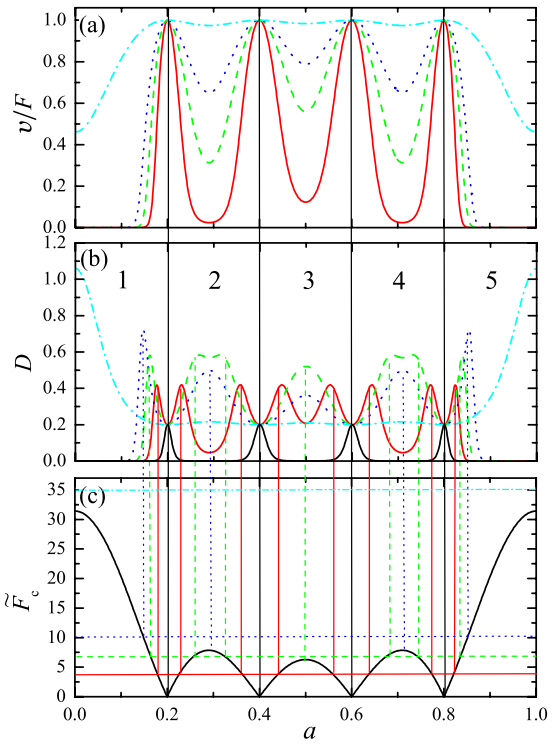

FIG. 4. (Color online) (a) Mobility v/F and (b) diffusion coefficient D from (22) for a system of $N=5$ rigidly coupled Brownian particles vs equilibrium interparticle separation a at different values of the tilt F. Solid red line, $F=4$; dashed green line, $F=7$; dotted blue line, $F=10$; dash-dotted cyan line, $F=35$. In (b), the solid black curve corresponds to the diffusion coefficient at zero tilt, $F=0$. All other parameter values are the same as in Fig. 1. (c) The critical force (30) corresponding to the effective potential (19). The four horizontal lines correspond to the above specified four values of the applied bias F.

large ensemble of the noninteracting system replicas, there will be a large spreading of velocities, resulting in the enhanced diffusion coefficient.

C. Dependence on the interparticle separation

If the strength of coupling between the constituents is weak, the effect of the equilibrium interparticle separation a on the diffusion properties is insignificant (cf. Sec. IV A and Fig. 4). Therefore, we will consider only the case of rigid coupling; for finite but still strong coupling between the particles, we numerically verified (not shown) that the main qualitative features discussed below are preserved.

In view of the symmetry property (24), we will focus on $a \in [0,L]$. Due to the invariance under $a \mapsto L-a$ it is in principle even sufficient to consider $a \in [0,L/2]$, but for the sake of better visualization of the essential features, the full range $a \in [0,L]$ will be plotted and discussed.

Figure 4 shows the velocity (a) and the diffusion coefficient (b) for a system of $N=5$ rigidly coupled Brownian particles as a function of a for several different tilt values. It is clear from Fig. 4(a) that the velocity as a function of a has four peaks, and these peaks become less and less pronounced as the tilt F is increased. With respect to the diffusion coefficient, it exhibits a more complicated multipeaked structure, Fig. 4(b): not only the positions and heights of the diffusion peaks, but also their number depend on the value of the applied tilt.

To understand this behavior, it is instructive to consider how the critical force corresponding to the effective periodic potential (20) depends on the interparticle separation a. It follows from Eqs. (20), (21), and (27) that the effective critical force is proportional to the amplitude $|\tilde{u}_1|$ of the effective potential:

$$\tilde{F}_c = \frac{4\pi}{L}|\tilde{u}_1| = \frac{\pi \Delta U}{LN}\left|\frac{\sin(\pi N a/L)}{\sin(\pi a/L)}\right|. \tag{30}$$

This dependence is shown in Fig. 4(c). The amplitude of the effective potential vanishes at $N-1$ values of $a=kL/N$, $k=1,2,\ldots,N-1$. Since the velocity of the system decreases with $\tilde{F}_c \propto |\tilde{u}_1|$ and attains the largest value $v_{\max}=F/\eta$ when $|\tilde{u}_1|=0$, to each zero of $\tilde{F}_c$ there corresponds a velocity maximum, and at each maximum of $\tilde{F}_c$ the velocity is minimized. For a system consisting of N particles, we therefore expect $N-1$ velocity maxima located at $a=kL/N$, $k=1,\ldots,N-1$.

For convenience of further discussion, we divide the whole domain of $a \in [0,L]$ into N equal regions of size L/N, with the kth region being defined as $[(k-1)L/N, kL/N]$, $k=1,\ldots,N$. For the special case $N=5$, these regions are marked with numbers in Fig. 4(b). In each such region, the dependence of $\tilde{F}_c$ on a has a single maximum. This maximum is located approximately in the "middle" of the regions with numbers $2,\ldots,N-1$, while in the first and the last regions, the maxima coincide with the region boundaries [see Fig. 4(c)]. The heights of the $\tilde{F}_c$ maxima in different regions, in general, are different.

At zero tilt value, $F=0$, the diffusion coefficient is maximized at exactly the same $N-1$ values of the interparticle separation as the velocity, i.e., at $a/L=1/N,\ldots,(N-1)/N$, where $D=T/(\eta N)$. For other values of a, the untilted periodic potential possesses barriers hindering the diffusive motion of the system. The dependence of D on a at zero tilt is shown in Fig. 4(b) as a solid black line.

For a small but finite value of the applied bias $F>0$, each of these maxima splits into two peaks. To understand this behavior, we note that for a small but finite bias, depending on the value of a, the system can be tilted either overcritically, or subcritically. The former situation is realized at those values of the interparticle separation a, for which $\tilde{F}_c(a)<F$, and the latter for $\tilde{F}_c(a)>F$. At each value of a where the effective critical force approximately equals the applied bias,

$$\tilde{F}_c(a) = F, \tag{31}$$

the system finds itself in a critically tilted potential, where the diffusion coefficient is maximized; see the discussion at the end of Sec. IV A. It is impossible to find the solution of Eq. (31) analytically for an arbitrary N, but graphically the solution corresponds to the intersection of the curve $\tilde{F}_c(a)$ with the straight line at the level of the tilt F [see Fig. 4(c)].

At small tilt values, we have $2(N-1)$ solutions of Eq. (31) in the domain $0 \leqslant a \leqslant L$, with two solutions in the $N-2$ middle regions, and one solution in each of the end regions with numbers 1 and N. Correspondingly, we have $2(N-1)$ maxima of the diffusion coefficient. In our numerical example, this situation is realized at $F=4$ (solid red line) in Fig. 4(b).

The N maxima of $\tilde{F}_c$ vs a in Fig. 4(c) are not of the same height: the one in the region 3 is somewhat smaller than those in regions 2 and 4, and the maxima in the end regions 1 and 5 are the largest. This means that for a tilt value slightly exceeding the maximal $\tilde{F}_c$ in region 3, but smaller than the maximal critical tilt in all other regions, the system is supercritically tilted in the third region at all values of a, whereas in other regions, it can be tilted either super- or subcritically, depending on a. Correspondingly, the two diffusion maxima in region 3 merge into a single one located at that value of a at which $\tilde{F}_c$ is the largest. In regions 2 and 4, the diffusion coefficient still has two maxima, approximately corresponding to the two solutions of Eq. (31) in those regions. This situation is realized at $F=7$ (dashed green line) in Fig. 4(b).

Upon further increase of the applied force F we enter the regime in which the system is overcritically tilted everywhere but in the end regions. Then, in the middle regions $2,\ldots,N-1$, we have a single diffusion peak, whose height gets smaller and smaller upon increasing the tilt. This situation is realized at $F=10$ and shown as a blue dotted line in Fig. 4(b). Only in the end regions 1 and N does Eq. (31) have a solution at a nonzero value of a, resulting in a diffusion maximum around that value.

Finally, at very large bias, Eq. (31) does not have a solution in any a-region and remains overcritically tilted for all values of a. The diffusion coefficient in this case has N rather small maxima, corresponding to N maxima of $\tilde{F}_c$ in each region [see Fig. 4(b), dash-dotted cyan line corresponding to $F=35$]. These maxima become less and less pronounced as F increases.

For $N>5$ one recovers analogous scenarios with essentially the same main features, while for $N<5$ some important features are missing.

V. CONCLUSIONS

We have investigated the behavior of N coupled, overdamped Brownian particles in a tilted periodic potential both analytically and numerically. Analytic results for the center of mass velocity and diffusion coefficient have been obtained in the asymptotic limits of weak and strong coupling by way of reducing the many-particle problem to an effective single-particle dynamics with renormalized temperature and periodic potential.

The dependence of the transport properties of the many-particle system on the tilt does not differ qualitatively from that in the single-particle case. At the same time, when viewed as functions of the coupling parameters, the velocity and diffusion coefficient exhibit several interesting peculiarities.

Due to the enhanced synchronization of the interwell transitions of the individual particles, both velocity and diffusion coefficient can be maximized with respect to the coupling strength. Furthermore, for sufficiently large coupling strengths, the velocity as a function of the equilibrium interparticle separation of an N-particle system exhibits $N-1$ maxima, while the number of maxima of the diffusion coefficient, as well as their positions and heights depend on the applied tilt. More precisely, there are $N-1$ diffusion maxima for zero tilt, while for small but finite tilt value, each of these maxima splits into two, resulting in $2(N-1)$ diffusion peaks. Further increase of tilt leads to sequential merging of the $N-2$ adjacent peak pairs, so that for sufficiently large bias, the number of diffusion peaks is N.

ACKNOWLEDGMENTS

We are grateful to Deutsche Forschungsgemeinschaft (Grant No. RE 1344/4-1 and SFB 613), the EUROCORES program FANAS of the European Science Foundation (CRP "Nanoparma"), and the EC Sixth Framework Program (Contract No. ERAS-CT-2003-980409) for financial support of this work.

[1] R. L. Stratonovich, Radiotekh. Elektron. (Moscow) **3**, 497 (1958) [English translation in *Non-linear Transformations of Stochastic Processes*, edited by P. I. Kuznetsov, R. L. Stratonovich, and V. I. Tikhonov (Pergamon, Oxford, 1965)].
[2] P. Reimann, C. Van den Broeck, H. Linke, P. Hänggi, J. M. Rubi, and A. Pérez-Madrid, Phys. Rev. Lett. **87**, 010602 (2001); Phys. Rev. E **65**, 031104 (2002).
[3] F. Jülicher, A. Ajdari, and J. Prost, Rev. Mod. Phys. **69**, 1269 (1997).
[4] P. Reimann, Phys. Rep. **361**, 57 (2002).
[5] A. Ajdari, J. Phys. I **4**, 1577 (1994).
[6] I. Derényi and T. Vicsek, Proc. Natl. Acad. Sci. U.S.A. **93**, 6775 (1996); Physica A **249**, 397 (1998).
[7] Z. Csahók, F. Family, and T. Vicsek, Phys. Rev. E **55**, 5179 (1997).
[8] S. Klumpp, A. Mielke, and C. Wald, Phys. Rev. E **63**, 031914 (2001).
[9] H.-Y. Wang and J.-D. Bao, Physica A **337**, 13 (2004); **357**, 373 (2005); **374**, 33 (2007).
[10] J. L. Mateos, Physica A **351**, 79 (2005).
[11] S. E. Mangioni and H. S. Wio, Eur. Phys. J. B **61**, 67 (2008).
[12] E. M. Craig, M. J. Zuckermann, and H. Linke, Phys. Rev. E **73**, 051106 (2006).
[13] J. Menche and L. Schimansky-Geier, Phys. Lett. A **359**, 90 (2006).
[14] S. von Gehlen, M. Evstigneev, and P. Reimann, Phys. Rev. E **77**, 031136 (2008).
[15] L. Prandtl, Z. Angew. Math. Mech. **8**, 85 (1928).

[16] G. A. Tomlinson, Philos. Mag. **7**, 905 (1929).
[17] A. E. Filippov, J. Klafter, and M. Urbakh, Phys. Rev. Lett. **92**, 135503 (2004).
[18] S. Maier, Y. Sang, T. Filleter, M. Grant, R. Bennewitz, E. Gnecco, and E. Meyer, Phys. Rev. B **72**, 245418 (2005).
[19] F. Family, H. G. E. Hentschel, and Y. Braiman, J. Phys. Chem. B **104**, 3984 (2000).
[20] O. M. Braun and Y. S. Kivshar, Phys. Rep. **306**, 1 (1998).
[21] M. Müser, in *Fundamentals of Friction and Wear on the Nanoscale*, edited by E. Gnecco and E. Meyer (Springer, Berlin, 2007), p. 177.
[22] H. D. Vollmer, Z. Phys. B **33**, 103 (1979).
[23] O. M. Braun, Phys. Rev. E **63**, 011102 (2000).
[24] O. M. Braun, R. Ferrando, and G. E. Tommei, Phys. Rev. E **68**, 051101 (2003).
[25] C. Fusco and A. Fasolino, Thin Solid Films **428**, 34 (2003).
[26] S. Gonçalves, V. M. Kenkre, and A. R. Bishop, Phys. Rev. B **70**, 195415 (2004).
[27] S. Gonçalves, C. Fusco, A. R. Bishop, and V. M. Kenkre, Phys. Rev. B **72**, 195418 (2005).
[28] X. R. Qin, B. S. Swartzentruber, and M. G. Lagally, Phys. Rev. Lett. **85**, 3660 (2000).
[29] E. Heinsalu, M. Patriarca, and F. Marchesoni, Phys. Rev. E **77**, 021129 (2008).
[30] A. Libál, C. Reichhardt, B. Jankó, and C. J. Olson Reichhardt, Phys. Rev. Lett. **96**, 188301 (2006).
[31] C. Lutz, M. Kollmann, and C. Bechinger, Phys. Rev. Lett. **93**, 026001 (2004).
[32] C. Lutz, M. Reichert, H. Stark, and C. Bechinger, Europhys. Lett. **74**, 719 (2006).
[33] K. Luo, T. Ala-Nissila, S.-C. Ying, and A. Bhattacharya, Phys. Rev. Lett. **100**, 058101 (2008).
[34] D. S. Fisher, Phys. Rev. B **31**, 1396 (1985).
[35] L. L. Bonilla, Phys. Rev. B **35**, 3637 (1987).
[36] A. V. Ustinov, M. Cirillo, and B. A. Malomed, Phys. Rev. B **47**, 8357 (1993).
[37] H. S. J. van der Zant, T. P. Orlando, S. Watanabe, and S. H. Strogatz, Phys. Rev. Lett. **74**, 174 (1995).
[38] P. Reimann, R. Kawai, C. Van den Broeck, and P. Hänggi, Europhys. Lett. **45**, 545 (1999); C. Van den Broeck, I. Bena, P. Reimann, and J. Lehmann, Ann. Phys.(Leipzig) **9**, 713 (2000).